INSTITUTE OF PHYSICS PUBLISHING PHYSICS IN MEDICINE AND BIOLOGY

Phys. Med. Biol. **47** (2002) 1–7 PII: S0031-9155(02)37737-6

Effect of ^{176}Lu background on singles transmission for LSO-based PET cameras

J S Huber[1], W W Moses[1], W F Jones[2] and C C Watson[2]

[1] Lawrence Berkeley National Laboratory, University of California, Berkeley, CA 94720, USA
[2] CPS Innovations, Knoxville, TN 37932, USA

Received 6 June 2002
Published DD MMM 2002
Online at stacks.iop.org/PMB/47/1

Abstract

We explore how the radioactive background from naturally occurring ^{176}Lu affects single photon transmission imaging for lutetium orthosilicate scintillator-based PET cameras by estimating the transmission noise equivalent count rate (NECR) including this background. Assuming a typical PET camera geometry (80 cm detector ring diameter), we use a combination of measurement and analytic computation to estimate the counting rates due to transmission, scatter and background events as a function of singles transmission source strength. We then compute a NECR for singles transmission. We find that the presence of radiation from the naturally occurring ^{176}Lu reduces the NECR by 60% or higher for source strengths less than 10 mCi, and that a 25% reduction of the NECR can occur even with a source strength of 40 mCi.

1. Introduction

Since its discovery approximately ten years ago (Melcher and Schweitzer 1992), cerium activated lutetium oxyorthosilicate or Lu_2SiO_5:Ce (LSO) has shown great promise as a PET scintillator because of its unique combination of short attenuation length, high light output and short decay time. The first PET scanner to utilize LSO is for imaging small animals (Cherry *et al* 1997, Chatziioannou *et al* 1999), but a large variety of PET detector modules utilizing LSO have since been completed or are under development (Fries and Bradbury 1997, Moses *et al* 1997, Pichler *et al* 1998, Schmand *et al* 1998, Correia *et al* 1999, Huber and Moses 1999, Saoudi and Lecomte 1999, Siegel *et al* 1999, Slates *et al* 1999). Another trend in PET instrumentation has been a renewed interest in 'singles transmission' for PET, where a ^{137}Cs source that emits single gamma rays (rather than a ^{68}Ge source that emits positrons) is used to obtain an attenuation map by performing what is essentially an x-ray CT scan. Attenuation correction in PET using a single photon transmission measurement has a higher count rate capability at the cost of additional scatter contamination, because conventional PET transmission using a positron source is limited by the near-side detector dead time (deKemp and Nahmias 1994, Karp *et al* 1995, Yu and Nahmias 1995, Bailey 1997,

Smith *et al* 1998). These two trends have converged, resulting in an LSO-based PET camera that employs a singles transmission source (Schmand *et al* 1998).

Despite its many advantages as a scintillator for PET, the lutetium in LSO contains approximately 2.6% ^{176}Lu, a naturally occurring radioisotope with a half-life in the order of 4×10^{10} years. This leads to a background count rate of approximately 240 cps/cc of scintillator material over the full spectrum (Melcher and Schweitzer 1992). This generates a negligible coincident background event rate, and so has been ignored in PET cameras. The purpose of this paper is to explore the effect of this background on the singles transmission measurement, which does not have the background rejection afforded by coincidence timing.

2. Methods

In order to quantitatively evaluate the effect of the ^{176}Lu background, we use the transmission noise equivalent count (NECR) metric (Strother *et al* 1990, Stearns and Wack 1993) that has been modified to include the ^{176}Lu background contribution, as the statistical error from the ^{176}Lu radiation lowers the NECR even after the average background rate is subtracted. The underlying assumption is that the quality of the transmission measurement depends only on the statistical accuracy of that measurement, and so two techniques that have the same NECR will produce equally accurate measurements when they accumulate data for the same length of time. We compute the NECR for singles transmission as

$$\mathrm{NECR} = \frac{Tr^2 L}{(Tr + S + LSO)} \tag{1}$$

where Tr, S and LSO are the transmission, scatter and ^{176}Lu background rates respectively and L is the system lifetime. No term for randoms is included, as it is not relevant for singles transmission. The transmission, scatter and background event rates all depend linearly on the front surface area of the detector module, so the relative fractions of these three rates are independent of the module front surface area for a given detector depth. We therefore quote rates for a single detector module assuming a 'typical' whole-body cylindrical PET camera with 80 cm diameter detector ring, a ^{137}Cs point source that orbits at a distance of 70 cm from the 'far' detector, and each detector module having a 51×51 mm^2 front surface. Changing the assumption to include more modules, different size modules, or multiple source geometries will not affect the conclusions, since all three rates (transmission, scatter and background) will scale by the same factor and so their ratios will be unchanged. Different assumptions for the ring diameter and source orbit diameter will change the results somewhat, as the ratio of background events to transmission events depends on these distances. Factors such as scintillator thickness and dead time can also affect this ratio—we determine our sensitivity to these parameters by computing the ratio given two different sets of assumptions for these values. We assume pre-injection transmission acquisition, so we have not included emission background contributions that can be significant for post-injection transmission acquisition.

Estimates of the flux of unattenuated transmission events on the detector module are based on geometrical factors and are multiplied by measured patient attenuation factors to predict the attenuated flux. More specifically, we use the source strength (including the 85% branching fraction for ^{137}Cs into a single gamma) and the geometry to compute the flux of (unscattered) gamma rays on the detector module. We multiply this flux by a patient attenuation factor, defined as the ratio (computed on a chord by chord basis) of the rates from the transmission scan and the blank scan. We consider two different values for the attenuation factor: the mean factor (i.e., the mean of all chords with a non-unity attenuation factor) and the maximum factor (i.e., the chord with the highest attenuation, typically from chords that pass through

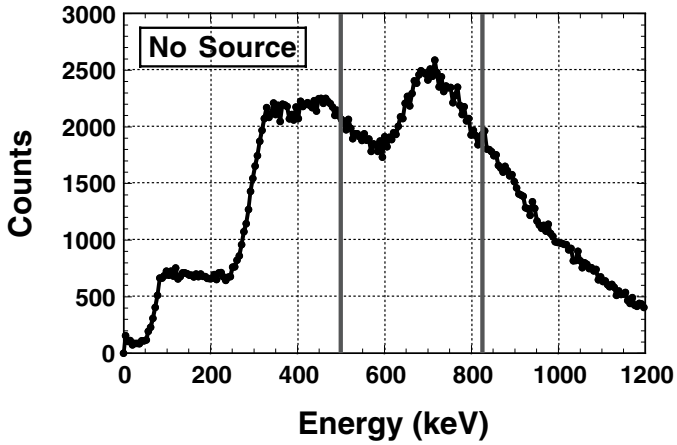

Figure 1. The natural background radiation spectrum of the LSO readout with photomultiplier tube. The total natural background activity is measured to be 241 cps/cc, with 99 cps/cc within a 25% energy window centered on the ^{137}Cs photopeak (i.e., 500–825 keV). The vertical bars indicate this ^{137}Cs photopeak window.

Table 1. Assumptions affecting the calculation for the estimated transmission and scatter event rates.

	Low performance	High performance
Dead time (paralyzing)	1000 ns	500 ns
Detector thickness	15 mm	30 mm
Scatter fraction (collimated)	6%	6%
Scatter fraction (uncollimated)	25%	20%
Photopeak efficiency	45%	73%

both shoulders). We have determined these factors from measured attenuation values in whole-body chest and thorax studies, and find a mean attenuation factor of 15 and a maximum attenuation factor of 74. Finally, we multiply this (attenuated) flux at the detector module by the photopeak efficiency, defined as the probability that an unscattered gamma ray impinging on a detector module results in a detected event. This includes the probability of absorption in the detector module, losses due to the 86% packing fraction (there is inactive volume due to the saw cuts in the scintillator and the light-tight can that surrounds the module) and the probability that an interaction results in a measured energy deposit that is within the 25% energy window of the readout electronics. Two detector module assumptions are explored: a 'low' and 'high' performance version, with the relevant assumptions for each shown in table 1. The values for virtually all detector modules in commercial, whole-body PET cameras are bracketed by these two assumptions.

To estimate the background rate from ^{176}Lu, we measure the self-activated pulse height spectrum from a $10.5 \times 10.7 \times 13.7\,\mathrm{mm}^3$ piece of LSO attached to a 2.54 cm square Hamamatsu 2497 photomultiplier tube. We plot the resulting spectrum in figure 1. The total background activity measured (i.e., the count rate, independent of the deposited energy) is 241 cps/cc, in agreement with previous measurements (Melcher and Schweitzer 1992, Ludziejewski 1995). Of this background, 99 cps/cc is within a 25% energy window centered on the 662 keV ^{137}Cs photopeak (i.e., 500–825 keV). This implies a 7.7 kcps

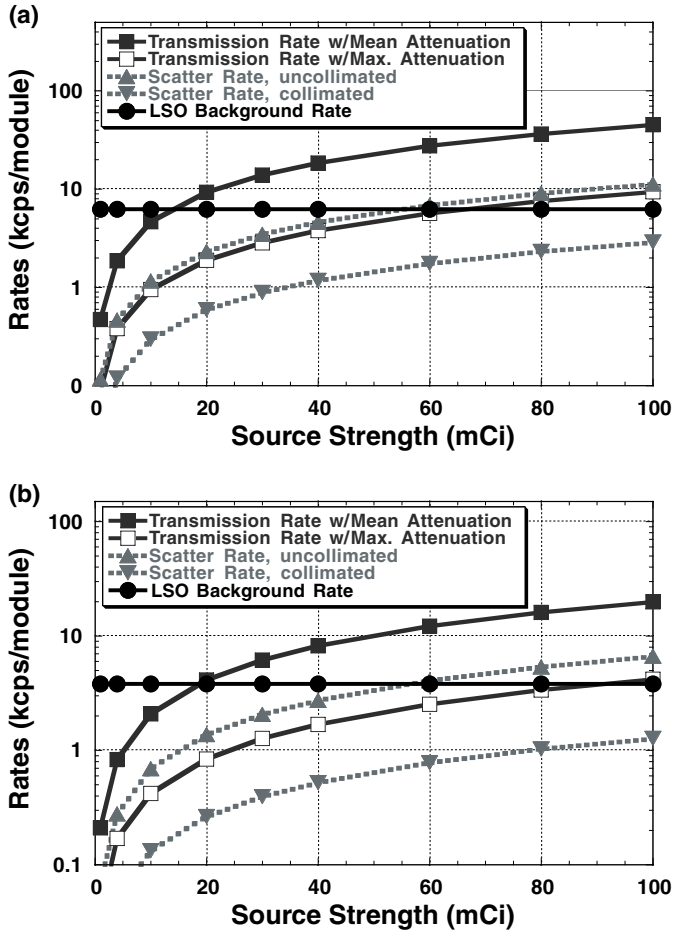

Figure 2. The estimated transmission, scatter and LSO background rates as a function of the source activity for a single detector module with (a) high and (b) low performance. The natural background radiation is greater than the mean transmission rate for sources less than 15 mCi (19 mCi) for the high- (low-) performance detector module.

^{176}Lu background rate within the ^{137}Cs photopeak for the high-performance detector module ($51 \times 51 \times 30$ mm^3 LSO) and a 3.84 kcps rate for the low-performance detector module ($51 \times 51 \times 15$ mm^3 LSO).

3. Results

Figure 2(a) shows the estimated transmission, scatter and LSO background rates, as a function of transmission source activity, for a single detector module using the high-performance detector assumptions described in the previous section. Note that the 7.7 kcps ^{176}Lu background rate dominates the total count rate for lower source strengths. To date, no PET camera has incorporated a singles transmission source with an activity above 20 mCi (Watson *et al* 1999, Karp *et al* 2000, Wienhard *et al* 2002) but this plot states that the background rate exceeds the mean transmission rate for source strengths below 15 mCi and the transmission rate at maximum attenuation for source strengths below 65 mCi. The

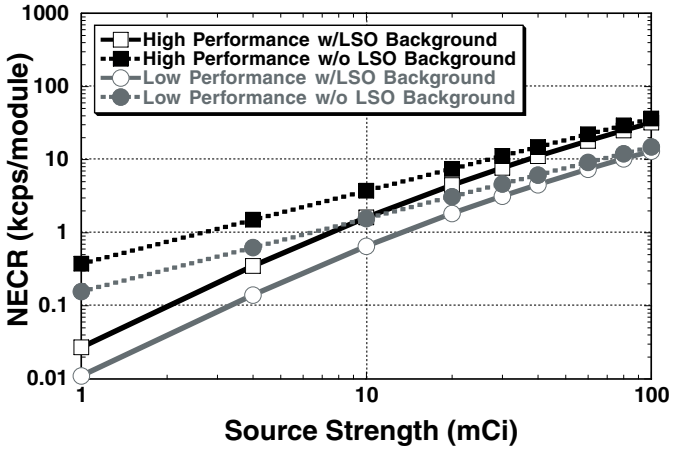

Figure 3. The transmission NECR for mean attenuation as a function of the source strength, shown for both high- (square) and low- (circle) performance camera detector modules obtained with (solid) and without (dashed) background from ^{176}Lu using an uncollimated source. The natural background radiation is seen to have a large effect on the transmission NECR at lower source strengths.

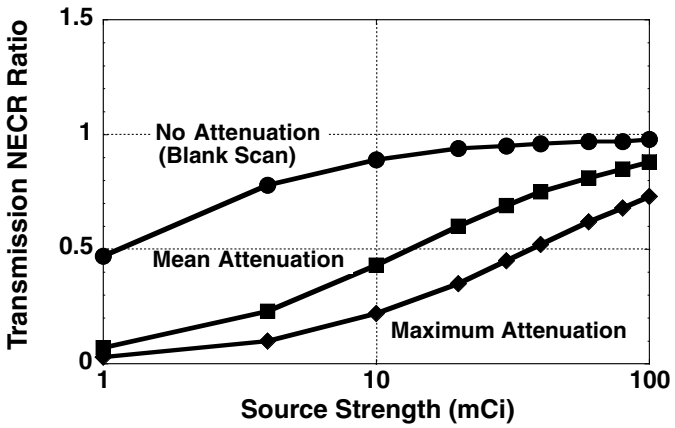

Figure 4. Transmission NECR ratio = transmission NECR with LSO/transmission NECR without LSO present, shown for high-performance camera with a range of attenuation levels using an uncollimated source. Natural background radiation has a large effect on the NECR particularly for maximum attenuation. The effect of the background is virtually the same for the low- and high-performance cameras (with an overall mean difference of less than 1%), so the low-performance data is not shown.

scattered event rates for both collimated and uncollimated transmission sources are a small fraction of the total event rate at all activities, implying that the effect of transmission source collimation can be neglected when evaluating the effect of the ^{176}Lu background. Figure 2(b) shows the same data for a low-performance detector module, demonstrating similar trends.

Figure 3 shows the transmission NECR as a function of transmission source strength for both the high- and low-performance modules. Also shown in this figure are the transmission NECR curves that would be obtained if there were no background from ^{176}Lu. A significant reduction in the NECR is evident, especially for lower source strengths.

Figure 4 shows the high-performance module data shown in figure 3, but re-plotted as the NECR with the ^{176}Lu background activity divided by the NECR without the background activity. This NECR ratio quantifies the factor by which the ^{176}Lu background 'degrades' the transmission data. Figure 4 implies that for mean attenuation and a 10 mCi source, the NECR with background is only 40% of that without background. This degradation factor is identical for the low- and high-performance assumptions (with an overall mean difference of less than 1%), suggesting that the effect of the background is nearly independent of the detector module assumptions.

Similar calculations (also plotted in figure 4) show that the effect of the background is not significant for the unattenuated ('blank') rate. The NECR blank scan with background and a 10 mCi source is 89% of that without background (i.e., NECR ratio = 0.89, see figure 4), implying that the NECR for the blank scan has decreased by 11%. Similar calculations show that the effect on coincidence data (including randoms) is negligible (not shown).

4. Discussion and conclusion

We have shown that the natural background radiation from ^{176}Lu has a significant effect when performing singles transmission. Figure 4 predicts that this background reduces the mean transmission NECR by a factor of 4.4, 2.3 and 1.4 when using 4, 10 and 40 mCi sources, respectively. Accurate prediction of the reduction in NECR obviously depends on the camera and patient attenuation factor, thus the effect should be calculated for the specific PET camera that will be used. However the reduction factors are independent of the module size, number of transmission sources and number of modules illuminated by each transmission source. They are virtually independent of a number of module performance factors (scintillator depth, dead time and photopeak efficiency) and transmission source collimation. They will depend on the ring diameter and source orbit diameter. We have provided estimates based on a wide range of detector module assumptions. This range brackets the range of these values likely to be found in whole-body PET cameras, so the results quoted should be generally applicable.

Figure 4 also predicts that the NECR for blank scans decreases by only 22%, 11% and 4% using 4, 10 and 40 mCi sources respectively for both collimated and uncollimated transmission data. Thus, the ^{176}Lu background has little effect on the blank scan but has a large effect on the singles transmission scan. Even with a 20 mCi source, the transmission scan time must increase by 67% to maintain the same level of signal-to-noise ratio obtained with a background-free scintillator.

These results suggest that single photon transmission imaging with a whole-body LSO-based PET camera requires a stronger source, as well as longer scan times, compared with conventional whole-body PET cameras. However, there are clearly practical limitations on how large the transmission source strength can be for clinical applications. Different shielding would be required to use $\sim$100 mCi sources because current shielding would not be adequate, and 'leakage' from such large transmission sources may affect the emission data. There might also be licensing and safety issues for these higher sources. Blank scans would have count rate issues if the camera is not designed to handle $\sim$1 Mcps per detector module.

We have assumed pre-injection transmission scanning in our calculations, which implies that there is no emission background contribution and maximal NECR. However, pre-injection transmission scanning can have significant drawbacks due to patient re-positioning in between the transmission and emission scans. Most transmission scans are currently done post-injection in clinical practice. Thus, the singles contribution from the emission activity can be as great or greater than the LSO contribution. In this case, the relative effect of the LSO on the NECR is less.

Acknowledgments

This work was supported in part by the Director, Office of Science, Office of Biological and Environmental Research, Medical Science Division of the US Department of Energy under contract no DE-AC03-76SF00098, and in part by the National Institutes of Health, National Cancer Institute under grant no RO1-CA67911 and National Institutes of Health, National Heart, Lung and Blood Institute under grant no P01-HL25840.

References

Bailey D L 1997 Strategies for accurate attenuation correction with single photon transmission measurements in 3D PET *Proc. Conf. on IEEE Nuclear Science Symp. and Medical Imaging (Albuquerque, NM, 1997)* ed O Nalcioglu pp 1009–13

Chatziioannou A F *et al* 1999 Performance evaluation of microPET: a high resolution LSO PET scanner for animal imaging *J. Nucl. Med.* **40** 1164–75

Cherry S R *et al* 1997 MicroPET: a high resolution PET scanner for imaging small animals *IEEE Trans. Nucl. Sci.* **44** 1161–6

Correia J A *et al* 1999 Development of a small animal PET imaging device with resolution approaching 1 mm *IEEE Trans. Nucl. Sci.* **46** 631–5

deKemp R A and Nahmias C 1994 Attenuation correction in PET using single photon transmission measurement *Med. Phys.* **21** 771–8

Fries O and Bradbury S M 1997 A small animal PET prototype based on LSO crystals read out by avalanche photodiodes *Nucl. Instrum. Methods* A **387** 220–4

Huber J S and Moses W W 1999 Conceptual design of a high sensitivity small animal PET camera with 4p i coverage *IEEE Trans. Nucl. Sci.* **46** 498–502

Karp J S *et al* 1995 Singles transmission in volume-imaging PET with a Cs-137 source *Phys. Med. Biol.* **40** 929–44

Karp J S *et al* 2000 Performance of a GSO Brain PET Camera *Proc. Conf. on IEEE Nuclear Science Symp. and Medical Imaging (Lyon, France, 2000)* ed J V Ulma Michele and Edward Hoffman pp 17/7–11

Ludziejewski T *et al* 1995 Advantages and limitations of LSO scintillator in nuclear physics experiments *IEEE Trans. Nucl. Sci.* **42** 328–36

Melcher C L and Schweitzer J S 1992 Cerium-doped lutetium oxyorthosilicate: a fast, efficient new scintillator *IEEE Trans. Nucl. Sci.* **39** 502–5

Moses W W *et al* 1997 Design of a high-resolution, high-sensitivity PET camera for human brains and small animals *IEEE Trans. Nucl. Sci.* **44** 1487–91

Pichler B *et al* 1998 Studies with a prototype high resolution PET scanner based on LSO-APD modules *IEEE Trans. Nucl. Sci.* **45** 1298–302

Saoudi A and Lecomte R 1999 A novel APD-based detector module for multi-modality PET/SPECT/CT scanners *IEEE Trans. Nucl. Sci.* **46** 479–84

Schmand M *et al* 1998 Performance results of a new DOI detector block for a high resolution PET-LSO research tomograph HRRT *IEEE Trans. Nucl. Sci.* **45** 3000–6

Siegel S *et al* 1999 Initial results from a PET planar small animal imaging system *IEEE Trans. Nucl. Sci.* **46** 571–5

Slates R *et al* 1999 Design of a small animal MR compatible PET scanner *IEEE Trans. Nucl. Sci.* **46** 565–70

Smith R J *et al* 1998 A comparison of segmentation and emission subtraction for singles transmission in PET *IEEE Trans. Nucl. Sci.* **45** 1212–8

Stearns C W and Wack D C 1993 A noise equivalent counts approach to transmission imaging and source design *IEEE Trans. Med. Imaging* **12** 287–92

Strother S C, Casey M E and Hoffman E J 1990 Measuring PET scanner sensitivity: relating countrates to image signal-to-noise ratios using noise equivalents counts *IEEE Trans. Nucl. Sci.* **37** 783–8

Watson C C *et al* 1999 Clinical evaluation of single-photon attenuation correction for 3D whole-body PET *IEEE Trans. Nucl. Sci.* **46** 1024–31

Wienhard K *et al* 2002 The ECAT HRRT: performance and first clinical application of the new high resolution research tomograph *IEEE Trans. Nucl. Sci.* **49** 104–10

Yu S K and Nahmias C 1995 Single-photon transmission measurements in positron tomography using Cs-137 *Phys. Med. Biol.* **40** 1255–66